1980LPSC...11.2159P

Proc. Lunar Planet. Sci. Conf. 11th (1980), p. 2159–2189.
Printed in the United States of America

Control of crater morphology by gravity and target type: Mars, Earth, Moon

Richard J. Pike

U.S. Geological Survey, Menlo Park, California 94025

Abstract—Both gravitational acceleration and target characteristics have influenced the shape of impact craters across the solar system. Contrasts in crater shape that are attributable to lithologic contrasts in their targets are evident for fresh craters on at least three planets, in decreasing order of certainty: Earth, the moon, and Mars. Observations available at this time suggest that the responsible differences in target characteristics involve layering rather than rock strength. Variations in target stratification may account for deviation of craters on Mercury, Mars, Callisto, and Ganymede from an inverse statistical relation between gravitational acceleration, g, and D_t, the mean diameter marking the transition from simple to complex craters. Callisto, Ganymede, and Mars are inferred to be weak or layered targets, whereas Mercury is inferred to be a strong or homogeneous target. Size-dependence of crater morphology on Mars, as determined from a new sample of 230 fresh craters from Viking Orbiter pictures, closely resembles that for lunar craters, except that D_t is about 6 km rather than about 19 km. Complex craters on Mars, which also have an unusually steep depth-to-diameter (d/D) trend, average 13 percent deeper on rough terrain than on plains. The simple-to-complex transition on Mars is paralleled by a change in the texture of ejecta from ballistic to fluid flow at D $\simeq$ 4 km, but the ejecta of large martian craters (>80 km) also has a primarily ballistic character. A revised analysis of data for the moon reveals that the simple-to-complex transition occurs in smaller mare craters than it does in upland craters: complex craters on the maria average 12 percent shallower than complex upland craters. Preliminary topographic data from Venus Pioneer radar suggest that possible impact craters on Venus could have a d/D ratio much like that of ringed complex meteorite craters on Earth.

INTRODUCTION

Impact craters are the outstanding surface features on solid planets (and satellites) in the solar system. Although the formational process—hypervelocity collision of a planet with much smaller bodies (asteroids, planetesimals, comet nuclei, meteoroids, and their fragments)—is thought to be essentially the same everywhere and over a wide range of impact energy, the resulting landforms are not all alike (e.g., Schultz, 1976). Impact craters can differ systematically in morphology by planet (Hartmann, 1972), location on a planet (Dence, 1972), size (Gilbert, 1893), and relative age (Baldwin, 1949). The contrasts in crater shape, some subtle and gradational but others blatant and abrupt, probably reflect one or more external influences on the impact process. These might include density,

© Lunar and Planetary Institute • Provided by the NASA Astrophysics Data System

1980LPSC...11.2159P

velocity, and angle of impact of the projectile; strength, structure, and physical state of the target material; the planet's gravitational acceleration, atmospheric density, and thermal history; and the efficacy of postimpact processes such as erosion, sedimentation, isostasy, and magmatism (Quaide *et al.*, 1965).

The many proposed influences on hypervelocity impact can be narrowed down to the most likely alternatives. One approach is measuring and otherwise documenting morphologic characteristics of freshly-formed impact craters and making interplanetary and intraplanetary comparisons of the findings. The work of Gault *et al.* (1975), Schultz (1976), Head (1976), Malin and Dzurisin (1977), Pike (1977), Smith and Hartnell (1978), Wood *et al.* (1978), and Mouginis-Mark (1979a) exemplify recent progress toward the goal. This paper elaborates on issues in crater morphology that I have previously raised only in abstracts and orally (Pike and Arthur, 1979; Pike *et al.*, 1980). It presents new results, primarily for Mars but including recent data for Earth and the moon as well, that deal with the possible influence of gravitational acceleration and target properties on the shape of impact craters. Older morphologic data for mercurian craters and recent (and preliminary) data for craters on Ganymede, Callisto, and (probably) Venus provide further context for the problems addressed here. The paper incorporates an emphasis that is absent in most current writing about impact craters: comparing terrestrial meteorite craters, the only readily available ground-truth, with impact craters on the planets (Dence, 1964; Von Englehardt *et al.*, 1967; Wilshire *et al.*, 1972; Milton *et al.*, 1972; Milton and Roddy, 1972; Roddy, 1979; Grieve and Robertson, 1979; Kieffer and Simonds, 1980).

PREVIOUS WORK

The interior morphology of freshly formed impact craters on a planet is more complicated with increasing crater size (Gilbert, 1893). This size/morphologic continuum is not perfectly gradational, but rather contains marked discontinuities or contrasts that can be used to evaluate some of the alternative influences on crater shape (Mackin, 1969). One of the two most evident contrasts is that between large craters and small basins. The other, that between simple and complex craters, is the aspect of crater shape described here. These observations apply primarily to fresh-appearing craters, because a surface morphology that is unaffected by postcratering degradation best reflects the formational processes that are of interest. Exactly what constitutes a "fresh" impact crater varies from study to study. However, the working definition current among planetologists, regardless of the precise criteria of selection, is a crater whose characteristics have changed little or none since formation. This definition is implemented here by criteria specified in the section on new martian data, below. I have assumed that the spirit of the definition has been adhered to by all workers whose morphologic data I have compared with mine.

© Lunar and Planetary Institute • Provided by the NASA Astrophysics Data System

1980LPSC...11.2159P

Simple and complex craters

Dence (1964) first recognized the fundamental and qualitative difference between simple and complex meteorite craters on Earth. The distinction was immediately applied to fresh-appearing impact craters on the moon (Quaide *et al.*, 1965). Although observations supporting the difference in crater shape are partly lithologic and structural for Earth but entirely topographic for the moon, they quite evidently describe the same phenomenon on both planets (e.g., Roddy, 1977). Simple lunar craters encompass Wood and Andersson's (1978) morphologic types ALC and BIO; complex craters correspond to their types TRI and TYC. The two-part classification, which was extended to include multiringed structures and basins on both Earth and the Moon (Dence, 1972; Hartmann, 1972) applies to impact craters on all six (observed) impacted bodies larger than Alamthea: Earth, the moon, Mars, Mercury, Ganymede, and Callisto.

The morphologic contrast is illustrated here for Mars. A simple crater (Fig. 1A) usually is a bowl-shaped depression that has a smooth and highly circular rim crest (C = 0.86 here; cf. Pike, 1977), an interior devoid of major topographic features, and a depth/diameter (d/D) or aspect ratio, of roughly 1/5 (I adopted the d/D notation of Wood and Andersson [1978] here rather than the R_iD_r notation of earlier publications [e.g., Pike, 1974], because of the need for the subscripted term D_t and because d/D is simpler). The upper wall of a simple crater commonly reveals stratification and evidence of mass-wasting. The crater may have a very small flat floor (although not in this example), presumably of mass-wasted debris (Pike, 1977) but possibly (on Mars) containing eolian sediment. A complex crater (Fig. 1B) has one or more of the following interior features: irregular or scalloped rim-crest outline, although still more or less radially symmetric; a broad floor that is flat and level overall, but that often is partly occupied or obscured by other morphologic features; a centrally disposed hill, peak, or pit; single or multiple slices or blocks of slumped material that may appear to have originally occupied scalloped segments in the upper wall of the crater; continuous terraces on the crater wall that represent wholesale failure of the rim *en bloc*; and a d/D that varies widely with diameter, from about 1/5 for small fresh complex craters to about 1/150 for large complex craters, depending upon the planet.

The simple-to-complex transition

Simple craters are small and complex craters are large. Morphologic studies have demonstrated that this generalization now applies to six planets and satellites (for example, Earth: Grieve and Robertson, 1979; the moon: Wood and Andersson, 1978; Mercury: Malin and Dzurisin, 1977; Mars: Carr *et al.*, 1977; and Ganymede and Callisto: Pike *et al.*, 1980). The transition from simple to complex morphologies may be expressed quantitatively. One of the more readily measured contrasts diagnostic of the transition is the change in d/D from about 1/5 to a lower and more variable fraction with increasing crater size.

© Lunar and Planetary Institute • Provided by the NASA Astrophysics Data System

1980LPSC...11.2159P

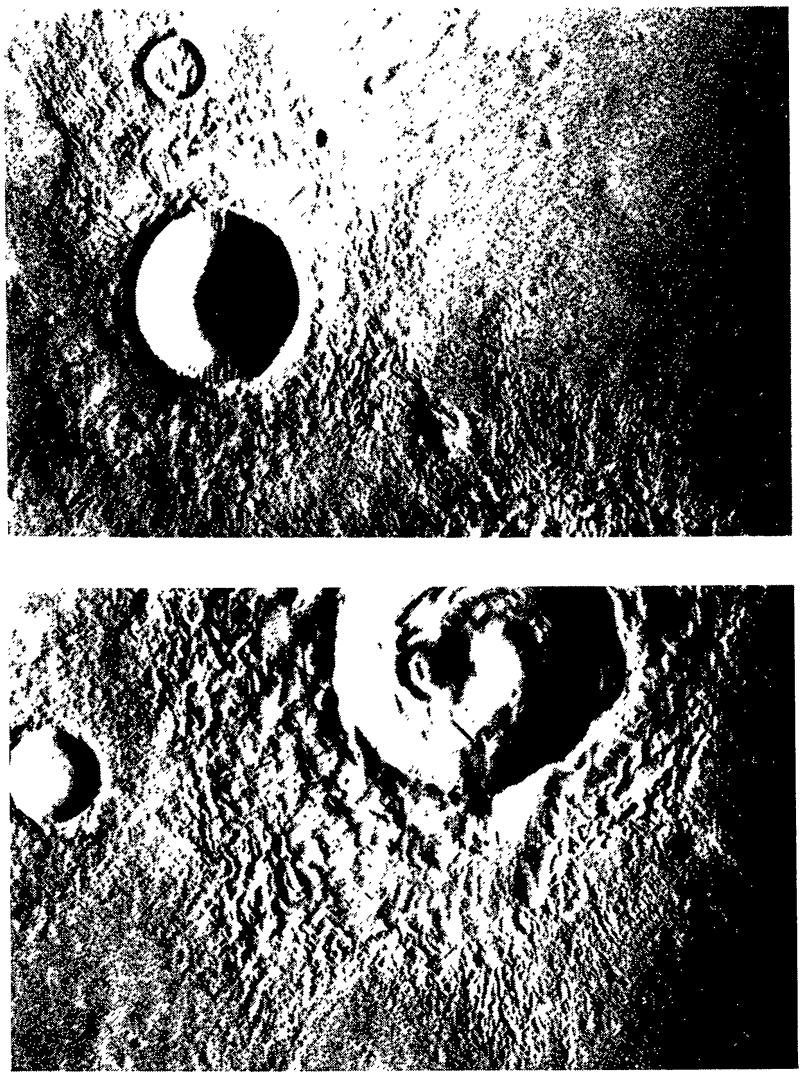

(a)

(b)

Fig. 1. (a) Fresh, simple impact crater on Mars at about 30°N and 264.5°W. One of the large (8.2 km across) and deep (1.9 km) simple craters in western Elysium Planitia discussed in text, it has the smooth, rounded interior typical of smaller simple craters and ejecta that shows characteristics of emplacement by fluid flow. Viking Orbiter frame No. 645A09. (b) Fresh, complex impact crater on Mars at about 31°N and 267.3°W, close to the simple crater pictured above. About 14.6 km across, it has a prominent central peak, scalloped rim crest, slump blocks, a small terrace, a comparatively modest depth (1.3 km), and a flat floor. Ejecta has well-developed flow characteristics: lobes and striations. Viking Orbiter frame No. 645A01.

The d/D results for fresh craters on four planets are summarized in Fig. 2; supporting data are given in Tables 1 and 2. A classification, into simple or complex, of all craters from which Fig. 2 is derived has been made for Mars (n = 230; Table 1), Earth (n = 30, Table 2), and the moon (n = 339, Table 2). The martian data, which are new, are discussed at length below. The d/D results of Pike (1974) for the moon are updated and improved here by adding more craters (largely from Pike, 1976) and by dividing the craters into simple and complex types *before* fitting the regression lines. These changes have been made to maintain a high-quality lunar data set that can be relied upon as a basis

© Lunar and Planetary Institute • Provided by the NASA Astrophysics Data System

1980LPSC...11.2159P

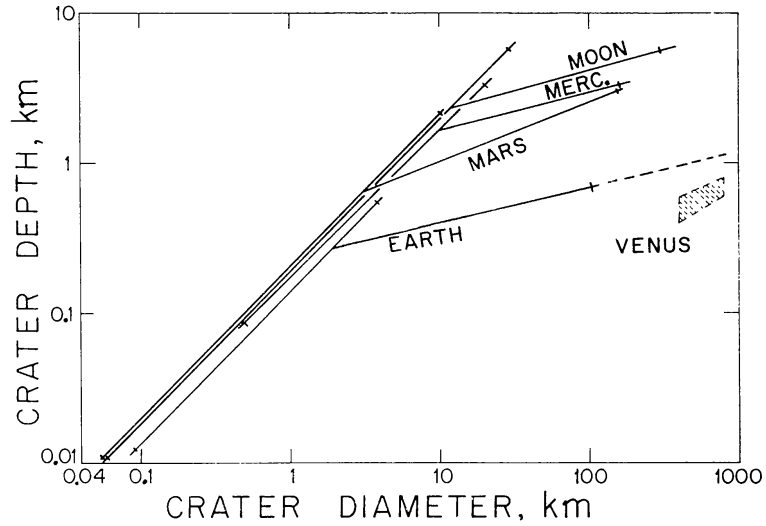

Fig. 2. Depth (d) vs. diameter (D) for simple (steep slope) and complex (gentle slope) impact craters on five planets. Lines are least-squares fits (Table 1, 2). Martian curves, undifferentiated by terrain type, are new from Viking Orbiter shadow-lengths (this paper); lunar curves are revised from those in Pike (1974) using data in Pike (1976); mercurian curves are from Malin and Dzurisin (1977); terrestrial curves mostly from data in Pike (1976); preliminary data for Venus from Pioneer Venus radar, reported by Kerr (1980).

Table 1. Depth/diameter for fresh impact craters on Mars: A summary of least-squares results.[1]

Terrain type	Crater type	Correl. coeff.	Sample size	Intercept (km)	Standard error (km)	Slope	± Std. error	Source
Mixed	Simple	0.96	21	0.187	+0.039, −0.032	0.962	0.064	2
Mixed	Complex	0.63	41	0.456	+0.098, −0.081	0.348	0.068	2
Mixed	Simple	0.92	49	0.162	+0.044, −0.035	1.003	0 063	3
Mixed	Complex	0.83	8	0.410	+0.047, −0.043	0.330	0.090	3
Mixed[5]	Simple	0.99	125	0.204	+0.025, −0.022	1.019	0.008	4
Plains	Simple	0.99	102	0.206	+0.024, −0.021	1.017	0.009	4
Cratered Terrain	Simple	0.99	23	0.195	+0.028, −0.024	0.999	0.024	4
Mixed[5]	Complex	0.93	105	0.415	+0.063, −0.055	0.395	0.016	4
Plains	Complex	0.90	51	0.467	+0.065, −0.057	0.334	0.023	4
Cratered Terrain	Complex	0.95	54	0.396	+0.058, −0.050	0.423	0.020	4

[1] Equations in form: log depth = log intercept + slope × log diameter
[2] Pike and Arthur (1979), photometric shadow lengths (data only)
[3] Pike *et al.* (1980), photogrammetry
[4] This paper, shadow lengths on Viking Orbiter prints
[5] Subdivided below by terrain type

© Lunar and Planetary Institute • Provided by the NASA Astrophysics Data System

1980LPSC...11.2159P

Table 2. Depth/diameter for fresh impact craters on four planets: A summary of least-squares results.[1]

Planet and terrain	Crater type	Correl. coeff.	Sample size	Intercept (km)	Standard error (km)	Slope	± Std. error	Source
EARTH	Simple	0.99	18	0.137	+0.029, −0.024	1.02	0.035	2
	Complex	0.68	12	0.23	+0.07, −0.06	0.24	0.08	
MERCURY	Simple	—	ca 80	0.176	— —	0.98	—	3
	Complex	—	ca 99	0.910	— —	0.26	—	
MOON								
Mare	Simple	0.99	179	0.195	+0.030, −0.026	1.013	0.008	2
Upland	Simple	0.99	89	0.192	+0.027, −0.024	1.022	0.009	2
Mare	Complex	0.94	24	0.841	+0.070, −0.065	0.332	0.025	2
Upland	Complex	0.92	47	1.008	+0.092, −0.084	0.313	0.020	2
PHOBOS	Simple	0.98	25	0.179	+0.060, −0.045	0.938	0.043	4

[1]Equations in form: log depth = log intercept + slope × log diameter
[2]This paper, data mostly from Pike (1976)
[3]Malin and Dzurisin (1977)
[4]Data from Thomas (1978, Fig. 20)

of comparison for craters on other planets. The craters used by Malin and Dzurisin (1977) in their d/D analysis for Mercury have not yet been formally classified into simple and complex types. Malin and Dzurisin's results are used in Fig. 2, however, because their selection criteria (1977, p. 377–378) seem to have been essentially those adopted here. Preliminary d/D measurements have been made for what appear to be a few large craters from Pioneer Venus radar data (reported in Kerr, 1980). The craters on Venus may not be as fresh as their presumably complex counterparts on other planets (Fig. 2). However, they evidently are fresh enough to have the strong relief that is needed for them to be detected in the orbiter's radar returns (only ~25 km horizontal resolution and 200 m vertical accuracy). Highly degraded craters on Venus probably would not show up on the results obtained from currently operational radar systems. These tentative data are included here because they are the first d/D estimates ever made for probable Venusian craters. Depth/diameter data for terrestrial meteorite craters (see Pike, 1976 and 1977) were compiled from many sources, most of which are cited in Grieve and Robertson (1979). All of the craters on Earth are at least slightly degraded, but this problem has been largely overcome, particularly for the small craters, by supplementing topographic data with information gathered from drill cores to get usable estimates of initial depth.

Figure 2 shows that simple craters on four planets are rather similar with respect to d/D, but that complex craters differ substantially. Fresh complex impact craters are deepest on the moon, followed by those of Mercury, Mars, and Earth, in that order. The diameter of intersection for each pair of curves can be used as one of several quantitative estimates for the location of the simple-to-complex transition of craters on that planet.

The transition from simple to complex morphologies is not abrupt, but rather is gradational over a modest crater-size range on each planet. Central peaks, flat floors, evidence for wall failure, and diminished d/D ratios do not all appear in complex craters at the same diameter. The transition may be expressed statistically as the geometric mean, D_t, of several diameter values that characterize

© Lunar and Planetary Institute • Provided by the NASA Astrophysics Data System

1980LPSC...11.2159P

specific morphologic contrasts (Pike *et al.*, 1980). Depth/diameter is but one of these. The other types of contrasts (Table 3) are exemplified by presence of swirl-textured floors in craters on the moon (modal diameter: Smith and Hartnell, 1978), observation of wall terracing in craters on Mercury (diameter at 50 percent frequency: Cintala *et al.*, 1977), craters displaying ballistic versus fluid-flow ejecta (median diameter of overlap: Boyce, 1979; this paper, Fig. 8), and occurrence of central uplifts in meteorite craters (median diameter of overlap: Grieve and Robertson, 1979; this paper, Fig. 4).

The salient result emerging thus far from the many studies of crater morphology is that mean transition diameter, D_t, is not the same on all planets. The difference is shown graphically in Fig. 3, a diagram that summarizes statistically the findings of various investigators (Table 3). Modified only slightly from the first version published in Pike *et al.* (1980), Fig. 3 furnishes a context for the new observations reported here. It also presents an interpretation of past morphologic results in terms of gravitational acceleration and target characteristics, insofar as any such general picture can be proposed at this time. Fig. 3 is fully explained in the caption.

The mean transition diameter, D_t, for impact craters on the four planets plotted as open circles in Fig. 3 varies roughly with the inverse of gravitational acceleration at the surface, g (both variables expressed logarithmically). The relation is approximate, for neither Mercury nor Mars falls on the regression line fitted to the four means. However, D_t values for Earth (3.1 km) and the moon (18.7 km) differ by a factor of six, exactly the ratio of their values of g. This correlation is too close to be accidental. The factor-of-six difference has been evident only since the detailed compilations of astroblemes by Dence (1972) and by Grieve and Robertson (1979) unequivocally established D_t for terrestrial craters as lying between 3 and 4 km rim diameter, and since Pike (1977) calculated D_t for the moon (revised here) as being at about 17.5 km.

Crater depth exemplifies individual variables that may scale inversely with g. From Fig. 2 and the equations in Table 2, it is evident that complex craters average six times deeper on the moon than they do on Earth. This already has been pointed out by Pike (1977), Cooper (1977), and by Grieve and Robertson (1979), and is discussed further by Pike (1980). I interpret the factor-of-six difference as indicating that crater depth could well scale inversely with g on all planets—allowing duly for perturbing factors to explain anomalies such as those of Mars and Mercury in Fig. 2. Venus may be a case in point. The recent d/D estimates for probable impact craters on Venus plot below the equation (which has a large dispersion) for terrestrial complex craters in Fig. 2. Thus, even if the data reported by Kerr (1980) represent somewhat degraded craters, these shallow features on Venus still could be roughly as deep as would be expected for a planet having a g similar to that of Earth, nearly 1000 cm/sec^2. Additional data are needed to test this possible d/D similarity between craters on Earth and their counterparts on Venus before any general dependence of impact crater depth on g can be affirmed.

There are at least two reasons for emphasizing the Earth-Moon relations in

© Lunar and Planetary Institute • Provided by the NASA Astrophysics Data System

1980LPSC...11.2159P

Table 3. Summary of morphologic data by which values of D_t were calculated for four planets.

Morphologic aspect	Statistic	Source	Sample size	Diameter (km)
		EARTH (8 morphologic aspects: D_t = 3.1 km)		
Overall transition	Median D overlap	Grieve and Roberston, 1979	80	3.5
Depth/diameter (d/D)	Intersection D of curves	This paper	30	1.9
Occurrence of simple craters:				
Crystalline rock	Largest D	Grieve and Robertson, 1979	31	4.5
Sedimentary rock	Largest D	Grieve and Robertson, 1979	35	2.4
Occurrence of complex craters:				
Crystalline rock	Smallest D	Grieve and Robertson, 1979	31	5.0
Sedimentary rock	Smallest D	Grieve and Robertson, 1979	35	2.5
Gravity anomaly/diameter	Intersection D of curves	Gordin *et al.*, 1979	29	4.0
Rim height/diameter	Intersection D of curves	Pike, 1976, and unpublished data	22	2.3
		MOON (23 morphologic aspects: D_t = 19 km)		
Overall transition	Misc. D (see p. 118 of source)	Mutch *et al.*, 1976	N.A.	20
Terraces/occurrence (maria)	50% frequency D	Smith and Hartnell, 1978	51	20
Terraces/occurrence (uplands)	50% frequency D	Smith and Hartnell, 1978	139	31
Types TRI + TYC/ALC+ BIO+TRI+TYC	50% frequency D	Wood and Andersson, 1978	2598	20
Swirl-textured floors/D	Modal D	Smith and Hartnell, 1978	221	25
Simple crater/occurrence	Largest D	Wood and Andersson, 1978	2598	27
Rimwall slope/diameter	Intersection D of curves	Pike, 1977	106	17
Rim-crest circularity/diameter	Inflection D of distribution	Pike, 1977	200	12
Rim-crest evenness/diameter	Inflection D of distribution	Pike, 1977	21	14
Cumulative morphology Index/D	Inflection D of distribution	Pike, 1975	152	9
Impact melt, exterior/D	Onset D of abundance	Hawke and Head, 1977	100	15
Apparent D/rim D	Intersection D of curves	R. J. Pike, unpublished data	144	15
Scallops/occurrence	Modal D	Wood and Andersson, 1978	2441	28
Central peaks/occurrence (maria)	50% frequency D	Wood and Andersson, 1978 Smith and Hartnell, 1978	N.A.	19
Central peaks/occurrence (uplands)	50% frequency D	Wood and Andersson, 1978 Smith and Hartnell, 1978	N.A.	27

© Lunar and Planetary Institute • Provided by the NASA Astrophysics Data System

Scallops + terraces (maria)	50% frequency D	Wood and Andersson, 1978	N.A.	19
Scallops + terraces (uplands)	50% frequency D	Wood and Andersson, 1978	N.A.	21
Overall transition	Onset D of terracing	Mackin, 1969	—	20
Depth/diameter	Intersection D of curves	Wood and Andersson, 1978	1534	12
Bowl shape/flat floors	50% frequency D	Wood and Andersson, 1978	2598	10
		Pike, 1975	152	
Rim height/diameter	Intersection D of curves	Pike, 1977	162	21
Rim width/diameter	Intersection D of curves	Pike, 1977	162	30
Floor diameter/D	Intersection D of curves	Wood and Andersson, 1978	1075	22
	MERCURY (18 morphologic aspects: D_t = 16 km)			
Rim height/diameter	Intersection D of curves	Cintala, 1979	30	16
Depth/diameter	Intersection D of curves	Gault *et al.*, 1975	130	9
Depth/diameter	Intersection D of curves	Malin and Dzurisin, 1977	178	10
Central peaks/occurrence	50% frequency D	Malin and Dzurisin, 1978	178	16
Central peaks/occurrence	50% frequency D	Gault *et al.*, 1975	130	11
Central peaks/occurrence	50% frequency D	Smith and Hartnell, 1978	152	12
Central peaks/occurrence (cratered terrain only)	50% frequency D	Cintala *et al.*, 1977	657	17
Central peaks/occurrence (plains only)	50% frequency D	Cintala *et al.*, 1977	336	20
Terraces/occurrence	50% frequency D	Gault *et al.*, 1975	130	12
Terraces/occurrence	50% frequency D	Smith and Hartnell, 1978	130	23
Terraces/occurrence (cratered terrains only)	50% frequency D	Cintala *et al.*, 1977	657	29
Terraces/occurrence (plains only)	50% frequency D	Cintala *et al.*, 1977	336	31
Overall transition	——	Malin and Dzurisin, 1977	178	10
Scallops/occurrence (cratered terrain only)	Modal D	Cintala *et al.*, 1977	657	25
Scallops/occurrence (plains only)	Modal D	Cintala *et al.*, 1977	336	25
Bowl shape (cratered terrain only)	50% frequency D	Cintala *et al.*, 1977	657	17
Bowl shape (plains only)	50% frequency D	Cintala *et al.*, 1977	336	19
Wall-failure	50% frequency D	Malin and Dzurisin, 1978	145	10

© Lunar and Planetary Institute • Provided by the NASA Astrophysics Data System

1980LPSC...11.2159P

Table 3. *(Continued)*

Morphologic aspect	Statistic	Source	Sample size	Diameter (km)
		MARS (10 morphologic aspects: D_t = 5.8 km)		
Depth/diameter	Intersection D of curves	This paper	230	3.1
Occurrence of simple craters	Largest D	This paper	125	10.2
Occurrence of complex craters	Smallest D	This paper	105	3.4
Ballistic-to-fluid-flow ejecta	Median D of overlap	This paper	230	4.1
Bowl shape to flat floor	Median D of overlap	This paper	230	6
Bowl shape to central peak	Median D of overlap	This paper	230	6
Bowl shape to slump blocks	Median D of overlap	This paper	230	6.5
Bowl shape to scalloped rim	Median D of overlap	This paper	230	6.5
Bowl shape to terraces	Median D of overlap	This paper	230	8
Bowl shape to peak pits	Median D of overlap	This paper	230	7.5

© Lunar and Planetary Institute • Provided by the NASA Astrophysics Data System

1980LPSC...11.2159P

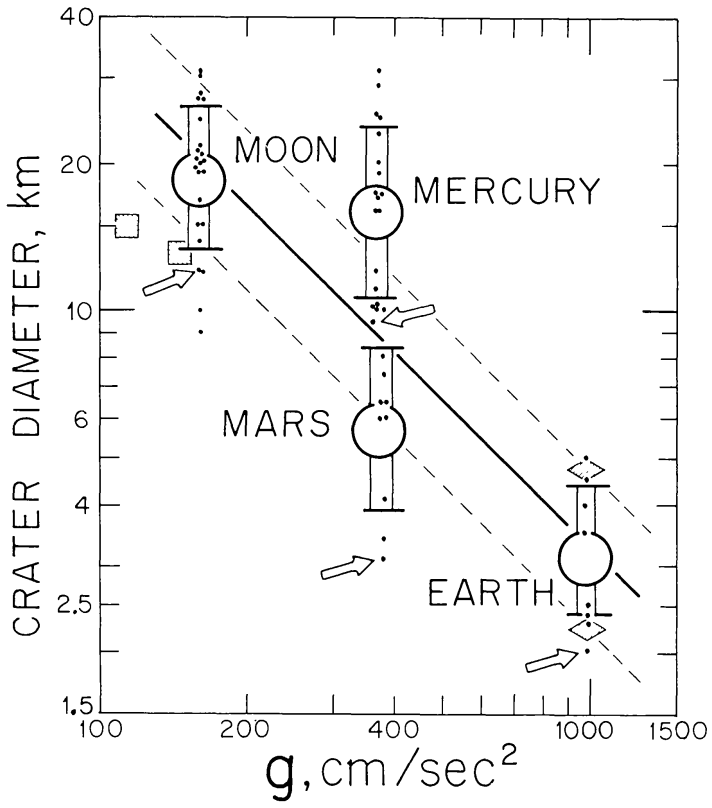

Fig. 3. The simple-to-complex transition for fresh impact craters on six planets and satellites, interpreted in terms of gravitational acceleration, g, and target characteristics. Each of the 59 small dots is a statistically derived crater diameter that expresses a different aspect of the transition, such as inflection of the depth/diameter distribution (arrows), frequency or onset of central peaks, and median overlap of simple and complex distributions (see text and Table 3). For clarity, the dots for Mars are displaced slightly to the right of those for Mercury. There are 23 morphologic aspects for the moon, 18 for Mercury, 10 for Mars (revised for this paper from Pike *et al.*, 1980), 8 for Earth, and one each (approximate onset of central peaks; see text and Pike *et al.*, 1980) for Callisto (upper square) and Ganymede (lower square). Large circles are centered on geometric means, D_t, for the 8, 10, 18, and 23 diameters of morphologic aspects for the four planets indicated. Bars show one standard deviation. Solid line, least-squares fit to four geometric means: $\log D_t = \log 3300 - 1.00 \log g$, interpreted as indicating targets of average strength or degree of stratification (see text). Slope of -1.00 is consistent with dimensionalities of plotted variables D_t and g. D_t value for Earth changes dramatically when craters are subdivided by type of target. Upper diamond: D_t for meteorite craters in crystalline rock only (see shaded rectangles in Fig. 4); lower diamond: D_t in sedimentary rock only (see Fig. 4). Dashed lines are extrapolations, down to lower values of g, of disparate terrestrial D_t values for crystalline and sedimentary rock, at a slope of -1.00: similar to slope of least-squares fit to the four whole-planet values of D_t. Upper dashed line interpreted to represent planets with resistant or homogeneous target characteristics. Lower dashed line interpreted to represent planets with weak or strongly layered targets. Martian data and estimates of D_t for impact craters on the two Galilean satellites are consistent with weak and layered, volatile-rich, strata (see discussion in text).

© Lunar and Planetary Institute • Provided by the NASA Astrophysics Data System

1980LPSC...11.2159P

Figs. 2 and 3 over the deviant D_t values for Mars and Mercury: (1) Lunar rocks (largely basalts, anorthosites, and their fragmental derivatives) have known terrestrial equivalents, whereas samples of rocks on Mars and Mercury have not yet been obtained. Indeed, the peculiar characteristics of crater ejecta on Mars suggest that the physical properties of rocks at the martian surface—whatever their composition—differ significantly from those on Earth, the moon, or Mercury. (2) Differences in crater shape that might be ascribed to characteristics of the space environment are less likely to occur on the earth and the moon than between these two bodies and Mars and Mercury. For example, the earth and its moon are so close to one another that they probably are not subject to significant differences in the velocity or mass-density distribution of impacting bodies, whereas these parameters conceivably could vary for more distant planets (Hartmann, 1977). For these reasons, I contend further that the deviation of Mars ($D_t \simeq 6$ km) and Mercury ($D_t \simeq 16$ km) from the solid line in Fig. 3 reflects influences on crater shape *in addition to* g, and thus does not necessarily disprove the dependence of D_t on g. One of these influences is geology (e.g., physical properties) of the target (Cooper, 1977; Cintala *et al.*, 1977; Wood *et al.*, 1978; Mouginis-Mark, 1979a; Kieffer and Simonds, 1980).

Target properties

The effects of lithology on diameter of the simple-to-complex transition are much better established for terrestrial meteorite craters than for craters on any other planet (Fig. 4). For other rock-correlated differences, see the recent review by Kieffer and Simonds (1980). From the compilations of data by Dence (1972) and Grieve and Robertson (1979), it is clear that the transition falls at a much smaller median diameter (about 2.25 km) for craters in sedimentary rock than for craters

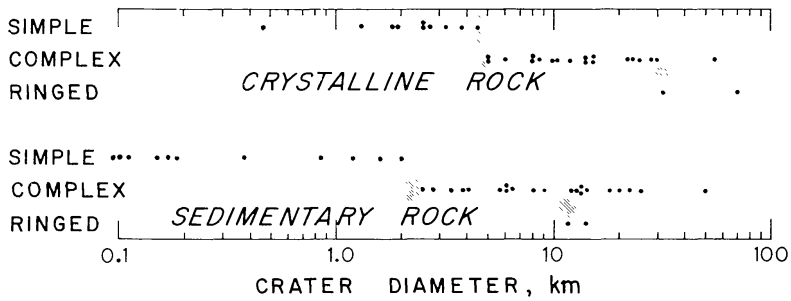

Fig. 4. Dependence of the simple-to-complex transition (essentially presence or absence of a central uplift) in terrestrial impact craters (shaded bars) on target characteristics. Transition in sedimentary rock occurs at D = 2.25 km, whereas it occurs at 4.75 km in crystalline rock. Transition from complex craters to ringed complex craters (shaded circles) exhibits similar trend. Comparison with lunar data in Fig. 9 suggests that the observed contrast in morphology reflects layering of the sedimentary targets rather than difference in overall rock strength. Arrays of "proven" and "probable" meteorite craters compiled from data of Grieve and Robertson (1979). N = 80.

© Lunar and Planetary Institute • Provided by the NASA Astrophysics Data System

1980LPSC...11.2159P

in crystalline rock (about 4.75 km). Although data on ringed impact structures that have been excavated wholly in either one type of target or the other are few (typical targets for these large craters being a veneer of sediments on a crystalline basement complex), the transition from complex craters to ringed structures also seems to depend upon rock type (Fig. 4).

Analogous contrasts in morphology have been sought in craters on other planets. The usual procedure is to examine craters on different topographic units, typically "smooth terrain" (maria and plains) and "rough terrain" (upland and cratered terrains) (Quaide *et al.*, 1965; Cintala *et al.*, 1977; Malin and Dzurisin, 1977; Smith and Hartnell, 1978; Wood *et al.*, 1978; Mouginis-Mark, 1979a) and to equate physiographic contrasts of the targets with differences in physical properties or structure. Results thus far indicate that target characteristics do indeed affect crater shape. Although intraplanetary differences can be pronounced, as they seem to be in the case of Mars (e.g., Mouginis-Mark, 1979a), the terrain-dependent results often are subtle, ambiguous, or even contradictory.

An example from the moon illustrates some of the problems with appraisals of terrain effects on the planets. According to equations 3–6 of Wood and Andersson (1978), fresh simple craters (their types ALC and BIO) on the lunar maria are 9 to 14 percent deeper (over the diameter range 2 to 20 km) than similar craters on the highlands, whereas my equations (Table 2) put the difference at less than half a percent. Both results cannot be correct. I contend that those of Wood and Andersson (1978) reflect a problem common to large samples of craters on planets with surfaces of greatly varying age. A sample of uniformly fresh craters can be obtained readily from surfaces that, as in the case of the lunar maria, are young. The task is much more difficult for rough, older terrains. Slightly older craters can easily be incorporated preferentially into a sample of fresh upland craters, which probably is what befell Wood and Andersson's sample of Class 1 (their freshest) craters for the lunar highlands. Older craters inadvertently find their way into highland samples because (1) the time-stratigraphic horizon that limits mare craters to exclusively young ones is absent from the older highlands surfaces, and (2) morphologic differences between Class 1 craters and the only slightly more degraded Class 2 craters can be subtle and difficult to judge on rough terrains. The statistical dispersion of crater depth calculated by Wood and Andersson (1978) bears out my thesis. Standard deviations, which are 56 percent (for Type ALC craters) and 78 percent (for Type BIO craters) greater on the uplands than on the maria, almost certainly reflect the inclusion of somewhat older and shallower craters in the upland sample. Thus it is clear that any terrain-related difference that might exist in the shape of fresh craters from different terrain categories can be masked by morphologic contrasts that reflect only relative age. Moreover, fresh impact craters can differ morphologically by virtue of having formed on uneven surfaces rather than on smooth surfaces, a contrast that is not necessarily related to physical properties of the target materials (Pike, 1977, Fig. 7; Wood and Andersson, 1978, p. 3676). A final caveat follows from this example. Namely, a large sample of craters emphatically does not guarantee either objectivity of the data or statistical validity of the results.

Just how lithology has brought about the factor-of-two difference in D_t on Earth is not known with certainty, but at least three (interrelated) aspects may be important: rock strength, stratification, and volatile content (see Kieffer and Simonds, 1980, and their extensive reference list). One possible explanation involves mainly rock strength and volatiles. On the basis of cratering experiments demonstrating that an impact of a given energy will generally excavate more efficiently in soft rock than hard rock (e.g., Cooper, 1977), Pike and Arthur (1979) suggested that the deviation of Mars and Mercury from the linear D_t:g relation (Fig. 3) might reflect crustal materials of significantly different strengths. They proposed that Mercury presented an unusually resistant target to an impacting body (upper dashed line in Fig. 3), compared to the moon and Earth—a conclusion foreshadowed, although not drawn explicitly, by the findings of Cintala *et*

© Lunar and Planetary Institute • Provided by the NASA Astrophysics Data System

1980LPSC...11.2159P

al., 1977), whereas Mars was a less resistant target (lower dashed line in Fig. 3). Wood *et al.* (1978) ascribed some *interior* morphologic features of complex martian craters to the presence of subsurface volatiles. Indeed, the results of cratering experiments (Cooper, 1977) demonstrate that water-saturated materials are much more easily excavated than dry materials. Thus the likelihood that the martian crust contains abundant volatiles (Carr *et al.*, 1977; Gault and Greeley, 1978; Cintala and Mouginis-Mark, 1980) is consistent with the weak-target interpretation for many of the data plotted in Fig. 3.

Preliminary estimates of the simple-to-complex transition for two Galilean satellites, both of which are believed to have largely water-ice crusts (see reviews by Morrison and Cruikshank, 1974; and Johnson, 1978), also are consistent with a weak-target interpretation of Fig. 3 (Pike *et al.*, 1980). The D_t values for Callisto and Ganymede in Fig. 3 were estimated solely from the prevalence of central peaks in small impact craters. I examined ten high-resolution (~3 km/line-pair) Voyager I images for each satellite, and on each picture measured the rim-crest diameter, D, of the three smallest craters for which a central peak could be seen with a 10X magnifier. This method probably estimates a characteristic crater size that is somewhat larger than the onset diameter for peaks because I could still detect peaks virtually at the limit of resolution (in craters as small as 8 km on Ganymede and 10 km on Callisto). The resulting median crater diameters, 15 km on Callisto and 13 km on Ganymede, fall only slightly below the weak-target model extrapolated to low values of g from terrestrial data in Fig. 3. Results from the 60 craters measured suggest that surface materials of the two Galilean satellites are even weaker than those of Mars. This is quite consistent with the subdued crater topography so clearly evident in the Voyager pictures (Smith *et al.*, 1979a and 1979b).

An alternative explanation of the data in Fig. 3, advanced here, is that stratification—or rather the degree of stratification—of the target and not its strength alone modifies the relation between D_t and g. The alternative follows from the inference that, for a given energy of impact, a complex crater will form more readily in a highly stratified target than in a homogeneous target (Roddy, 1977; Cooper, 1977). The overall concept is not new. A layered target, albeit *specifically* consisting of unconsolidated material overlying bedrock, has been invoked to explain flat floors and central peaks in impact craters for some time (Wegener, 1921; Sabaneyev, 1962; Oberbeck and Quaide, 1967; Head, 1976). I propose here (1) that stratification can merely *determine* (and as a factor distinctly subordinate to g) the crater *size* at which the complex features appear (Fig. 4), *not initiate* the features themselves (Pike, 1980), as Wegener (1921) and those who adopted his model maintained. Moreover, (2) just what constitutes a layered target needs to be clarified and broadened: a stratified target need not consist exclusively of a weak surface layer and a strong substrate, as currently seems to be the working definition in planetary studies. Stratified targets on Earth often comprise alternating beds of (weak) sedimentary rock, with varying degrees of strength. The sedimentary sequence often is thick enough so that the underlying basement complex of (strong) crystalline rock does not impinge upon formation of the impact crater. Well-known complex craters excavated in targets of this type include Flynn Creek, Tennessee (Roddy, 1979), Steinheim Basin, Bavaria (Von Englehardt *et al.*, 1967), and Sierra Madera, Texas (Wilshire *et al.*, 1972). Some

© Lunar and Planetary Institute • Provided by the NASA Astrophysics Data System

1980LPSC...11.2159P

extraterrestrial layered targets may be somewhat similar. For example, sequences of lava flows alternating with eolian, fluvial, or glacial sediments could well have accumulated on Mars, and layers of ice, interspersed with deposits of impact ejecta, may comprise much of the upper crusts of Callisto and Ganymede.

The diversity of crater morphology revealed by Viking Orbiter pictures (Carr *et al.*, 1977) suggests that detailed analysis of martian craters on contrasting terrains might assist in choosing between rock strength and rock layering, or otherwise contribute toward eventual solution of the simple-to-complex problem. Indeed, some general terrain-related effects on crater morphology on Mars already have been identified (Wood *et al.*, 1978; Johansen, 1979; Mouginis-Mark, 1979a). I have examined the morphology of fresh-appearing martian craters for which rim-to-floor depth (d) and rim diameter (D) could be measured from Viking Orbiter data. The first results were published for 73 craters where d/D data were extracted by a detailed photometric technique (Pike and Arthur, 1979). Related findings for 57 craters where d/D measurements came from photogrammetry have appeared more recently (Pike *et al.*, 1980). This paper presents the results of the most recent survey of martian craters, those whose depths were measured from shadow lengths on Viking Orbiter prints.

THE NEW DATA

Criteria

The 230-crater sample analyzed here (Fig. 5) resulted from a systematic perusal of all enlarged (six-inch) Viking Orbiter prints (shade-corrected versions only) in the U.S. Geological Survey Menlo Park file in February 1979. Except for some of the earlier spacecraft revolutions, the collection was relatively complete through frames A900 and B705. In order to obtain consistent and reliable data on crater depth/diameter as well as on photogeologic characteristics, stringent standards for both image quality and crater suitability were maintained. Criteria of selection included image clarity and resolution, sun-elevation angle and sun azimuth, shadow density and length, and freshness of the crater form. Comparatively few of the thousands of available pictures, especially those covering high latitudes, proved suitable for both measurement of crater depths and identification of diagnostic morphologic features.

Only fresh craters were accepted so that the analytical results would be comparable to those for craters on the moon (Pike, 1974; Wood and Andersson, 1978) and the other planets (e.g., Malin and Dzurisin, 1977; Smith and Hartnell, 1978). Selection of the sample was intentionally biased toward fresh craters, although I did not erect a formal relative-age classification such as used by Baldwin (1949) or by Wood and Andersson (1978). In the spirit of the discussion earlier in the paper, I defined freshness of crater form as overall crispness of the rim and other interior morphologic features, minimal superposition of much smaller impact craters on both the interior and on the ejecta blanket, and where resolvable, presence of fresh-appearing ejecta. Otherwise fresh-appearing craters that

© Lunar and Planetary Institute • Provided by the NASA Astrophysics Data System

1980LPSC...11.2159P

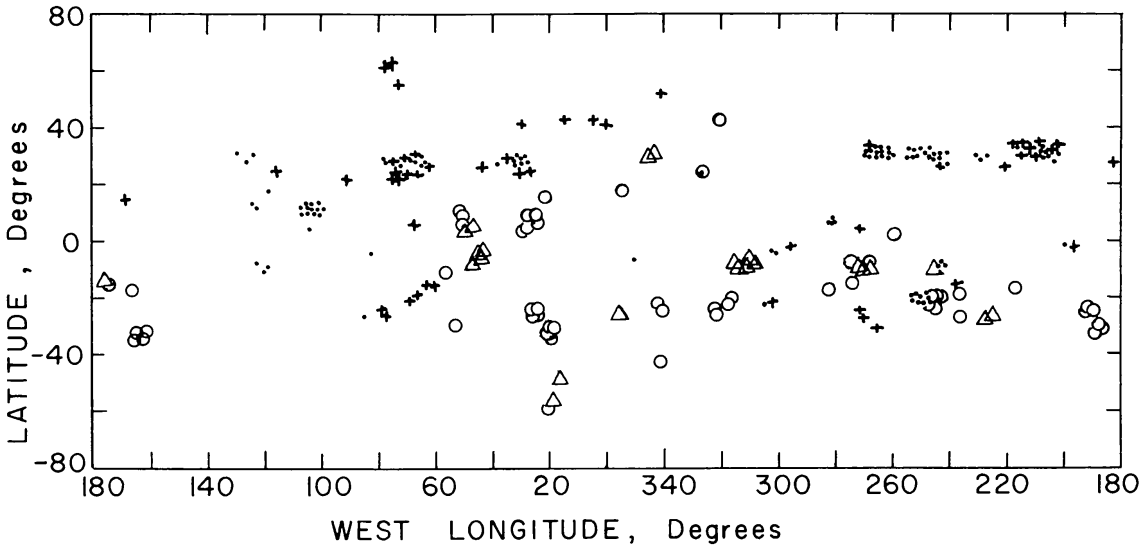

Fig. 5. Areal distribution of the 230 martian impact craters. Concentrations of symbols indicate coincidence of high-quality images with occurrence of fresh craters in this sample. There are 102 simple craters on plains (dots), 23 simple craters on cratered terrain (triangles), 51 complex craters on plains (crosses), and 54 complex craters on cratered terrains (circles). For distribution by photogeologic units see Table 4; for distribution by size (rim diameter, D) see Fig. 6.

seemed to contain significant fill (for example, an unduly broad flat floor that embayed and partially buried the central peak or pit) were omitted. Age of the photogeologic unit (Scott and Carr, 1978) on which the crater was located was not a criterion.

Resolution and image quality had to be sufficient for an unambiguous classification of a crater as either simple or complex and for clear evidence of either ballistic or fluid-flow textures (for this distinction, see Carr *et al.*, 1977) in the ejecta. For example, craters that were obviously large enough to contain peaks, terraces, and other complex features (see Fig. 7, below), but both lacked these features *and* also appeared only on low-quality images, were rejected. In order to obtain the best possible d/D data, and following lunar practice, I rejected simple craters for which the sun-elevation angle fell below 15° or exceeded 25°. Somewhat lower sun angles were often accepted for large complex craters to insure that the shadow tip extended onto the flat floor. In no case were sun angles higher than 30° or lower than 10° permitted. Considerable experimentation showed that crater depths derived from outside these limits often were unreasonably low or high (e.g., depths for simple craters that yielded a d/D of 0.4; twice that evident for fresh lunar craters). Because anomalously high or low depths also resulted from some pictures where the sun azimuth departed significantly from 90° or 270°, deviations of more than two or three degrees from due east or west were cause for rejection of a picture. I do not yet understand this effect, but mention it to indicate the care taken to exclude all possible sources of error from the data. The shadows cast in crater interiors had to be dense and sufficiently crisp to permit unambiguous measurement of their lengths. Moreover, any substantial difference between shadow configuration in orthographic and rectilinear versions of the prints, which could indicate false "shadows" resulting from manipulation of the grey scale during image processing, prompted rejection of the crater. Finally, shadow margins in simple craters had to lie at, or approximately at, the center of the crater (18 exceptions discussed below) and had to be smoothly rounded, not squared off. An important exception to the latter rule applies to those obviously otherwise simple craters that had very small flat floors (e.g., Pike, 1977; Wood and Andersson, 1978). Edges of the broad, squared-off shadows typically observed in complex craters had to be cast from the rim crest onto the flat floor, and not from a high rimwall terrace or onto a terrace located part-way up the inner wall. The above criteria excluded many otherwise suitable martian craters from the sample.

© Lunar and Planetary Institute • Provided by the NASA Astrophysics Data System

1980LPSC...11.2159P

The data

The size of the new sample for Mars is comparable to that used to establish the d/D relation of fresh lunar craters from Apollo data (Pike, 1974). Morphologic data on most of the 230 martian craters that survived all the tests for exclusion should gain in both precision and accuracy what they lack in sheer volume. There are some exceptions. Data on 39 simple craters less than 0.9 km across—roughly the limit of resolution for identifying morphologic features in craters on the bulk of the Viking Orbiter images—are far less precise and complete than data on larger craters. These small craters were included to extend the d/D relation down to as small a crater size as possible. Virtually no morphologic information is available on the under-0.9 km-diameter craters, although all of them probably have the simple morphology. A pocket optical comparator sufficed to measure diameters and shadow lengths for such craters, the smallest of which were only about two or three pixels across. The craters for which depth and diameter were determined range from D = 53 m and d = 10 m to D = 155 km and d = 3.23 km. Diameters were calculated from the SEDR data sheets and edge data rather than from the printed bar scales, which cross-checking revealed were occasionally incorrect (M. H. Carr and D. W. G. Arthur, pers. comm., 1979–1980). As for complex craters on the moon (Pike, 1976), depths of complex craters on Mars are average values, not maximum figures from the longest shadows.

Depths for 18 especially well-depicted simple craters on high-resolution images in which the shadow tip did not strike the exact crater center, usually (but not always) the lowest point, were adjusted upward empirically. This was done because eight of the craters were of the large simple type discussed below, and thus of special interest. The correction, which relates percentage of crater depth to percentage of crater radius covered by shadow, was derived from the averaged interior geometry of four fresh simple craters on the moon (Macrobius A and B, Cauchy CA, and a small unnamed crater on map 40A4S1) that are particularly well contoured on Lunar Topographic Orthophotomaps. The average increase in crater depth was about 18 percent of the value measured from Viking Orbiter pictures. Because the interior form of the fresh *simple* craters differs little from planet to planet (Fig. 2), the lunar-based correction introduced little or no subjectivity into the martian sample. Validity of the procedure is confirmed indirectly by the fact that omission of the 18 depth-corrected craters does not change the d/D equations for simple martian craters (Table 1).

In addition to depth and diameter, I ascertained the presence of the following nine morphologic features described earlier (cf. Fig. 1A and 1B): bowl shape, flat floor, central peak (or central depression), "slump" block, scalloped rim crest, rimwall terrace, cratered central peak (peak pit), predominantly ballistic ejecta, and predominantly fluid-flow ejecta. In some few cases, identification of one or two of these features is uncertain, owing to marginally acceptable resolution, poor development or uncertain expression of the feature, or obscuration of a possible feature by interior shadow.

Crater classification

Before analyzing the data, the 230 craters (Fig. 5) were grouped as to photogeologic background on Mars, either plains (n = 153) or rough (cratered) terrain (n = 77, and overall morphologic type, either simple (n = 125) or complex (n = 105). Craters in the plains subset fall on nine of the geologic units mapped by Scott and Carr (1978), all but one of which (unit Npm) are of Hesperian age or younger (Table 4). Most (79) of the plains craters are on one of the youngest terrains, unit Apc. Craters in the cratered-terrain subset fall on four of Scott and Carr's Noachian-age map units (Table 4). All but two of these craters are located on unit Nhc and Nplc, old heavily-cratered terrain in the uplands. The definition of a simple crater is fairly conservative, and usually requires a crisp, rounded shadow tip on a bowl-shaped and clearly featureless bottom. Most departures from this elementary form identify a crater as complex. The presence of a small flat floor, which because of its often multigenetic character is not a diagnostic criterion of morphologic complexity, can be an exception to this rule of crater taxonomy (see Pike, 1977 and Wood and Andersson, 1978). In practice, grouping the fresh impact craters in this sample as either simple or complex was not difficult. Other classifications of complex martian craters are, of course, possible (e.g., Johansen, 1979; Mouginis-Mark, 1979a).

© Lunar and Planetary Institute • Provided by the NASA Astrophysics Data System

1980LPSC...11.2159P

Table 4. Photogeologic terrain type of 230 fresh craters on Mars.[1]

n	Symbol	Possible or probable geology
		PLAINS MATERIALS
		(Mostly Amazonian and Hesperian in age)
6	Aps	Eolian and volcanic materials
1	Apt	Young lava plains
15	Avy	Young basaltic lava flows
79	Apc	Eolian-veneered lava plains
23	Hpr	Lava plains
1	ANch	Fluvial and eolian deposits
17	Hprg	Volcanic flows
10	Hvo	Shield volcanoes and flow units
2	Npm	Cratered lava plains
		ROUGH (CRATERED) TERRAIN MATERIALS
		(Mostly Noachian in age)
1	HNk	Diverse origins
39	Nplc	Ancient lava flows and impact ejecta
1	HNbr	Ejecta and ancient terrain
35	Nhc	Oldest exposed surface on Mars

[1] After Scott and Carr (1978).

GENERAL RESULTS

An analysis of the new martian data is presented in Figs. 2, 3, 6, 7, and 8, and in Table 1. The findings are consistent with the overall picture of size-dependence in crater morphology that was outlined previously (Pike and Arthur, 1979; Pike *et al.*, 1980). The diameter of the simple-to-complex transition, D_t, for fresh craters on all terrain types has been recalculated (Fig. 3). The D_t for Mars now is 5.75 km (n = 10 variables), down from the 6.3 km value of Pike *et al.* (1980) and the nearly 7 km value of Pike and Arthur (1979), a trend that reflects increasing attention to detail and better sampling of craters on Mars. I do not expect this figure to decrease much further. The new D_t value does not disrupt the inverse relation between crater morphology and gravity-cum-target strength (or layering) (Fig. 3). In fact, the data point for Mars now is a better fit to the line extrapolated back from terrestrial impact craters in sedimentary rock. The other, more specific new results are addressed below.

INTERIOR MORPHOLOGY

Depth/diameter results

Linear depth/diameter fits (Table 1) to all 230 craters are roughly equivalent to those derived previously for smaller samples (Pike and Arthur, 1979; Pike *et al.*, 1980). The new expressions differ from the most recent results of Cintala and

© Lunar and Planetary Institute • Provided by the NASA Astrophysics Data System

1980LPSC...11.2159P

Mouginis-Mark (1980) in that their trend for large (equivalent to my complex) craters is much steeper than mine and their equation for small (my simple) craters is somewhat lower and less steep than mine. All in all, fresh simple craters on Mars have about the same interior geometry (d/D) as fresh simple craters on other solid planets (Fig. 2). It is also clear from the equations plotted in Fig. 2 that complex martian craters, which fall midway between those on the moon and Mercury and those on Earth (and perhaps Venus), have a much steeper d/D relation (slope = 0.395) than is observed elsewhere in the solar system (0.24–0.332). Cintala and Mouginis-Mark (1980) offered one possible explanation for this, probably real, steepness in terms of substrate volatiles.

Terrain-correlated differences in martian craters are ambiguous with respect to depth/diameter. The new results for Mars are broken down by terrain and crater type in Figure 6 and in Table 1. The two sets of log-linear distributions have much in common. In both cases the transition from simple to complex craters occurs at about 3.5 km diameter. However, the equations for craters on plains units cross at a crater diameter of 2.5 km, whereas they intersect at 3.3 km for craters on the rough terrains. The difference may be significant, but conceivably could reflect too small a sample. Simple craters on the plains also are about five percent deeper than those elsewhere on the planet, a small difference that may

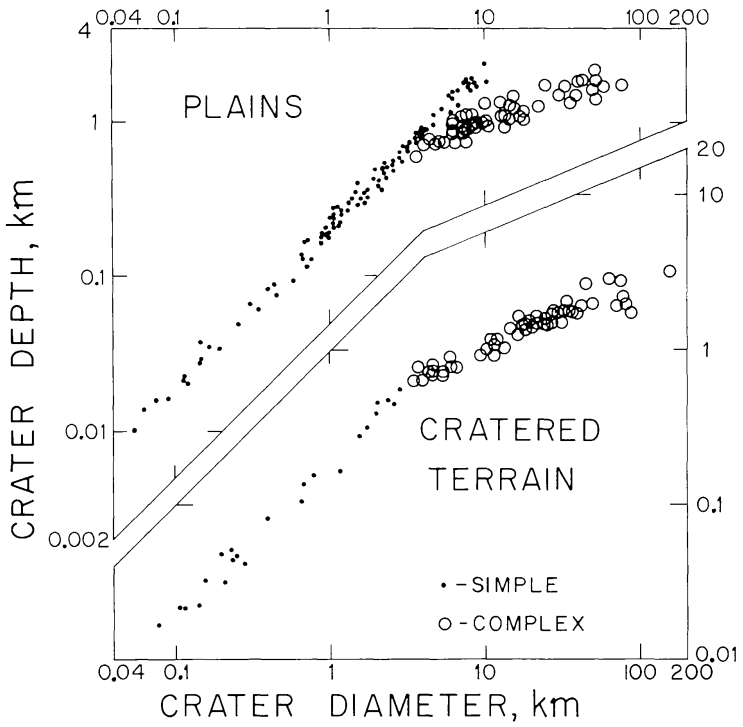

Fig. 6. Depth/diameter results for 230 fresh martian impact craters illustrate the morphologic transition from simple to complex. Simple craters on cratered terrains (n = 23) are no larger (3.4 km across) than the smallest complex craters (n = 53), whereas simple craters on plains (n = 102) reach diameters (maximum = 10.3 km) well beyond that (3.6 km) of smallest complex craters (n = 52). Depth/diameter equations (Table 1) differ considerably more for complex craters than for simple craters. Depths measured from shadow lengths on Viking Orbiter pictures.

© Lunar and Planetary Institute • Provided by the NASA Astrophysics Data System

1980LPSC...11.2159P

reflect nothing more than the previously cited tendency for slightly older and more degraded craters to be incorporated into crater samples from rough, old terrains (cf. Table 2, Fig. 9; Pike, 1974; and Wood and Andersson, 1978, p. 3676). The d/D distribution for complex craters in rough terrains has a steeper slope (0.423) than that for the plains (0.334), although nowhere near the 0.557 observed by Cintala and Mouginis-Mark (1980) from their d/D data. Complex craters on plains also are shallower than those elsewhere on Mars. The difference between the two equations (Table 1) varies from zero at D = 5 km to about 27 percent at D = 100 km. Moreover, the considerable scatter for both subsets of complex craters suggests caution in making geologic conclusions based on these contrasts. The most convincing difference between fresh impact craters on the two principal types of martian terrain may lie not in the d/D equations themselves but rather in the fact that simple craters on the plains extend well past the intersection diameter, to about 10 km D, whereas such large simple craters are absent from cratered terrains.

Other interior features

Size-morphology arrays for nine geomorphic aspects of crater interiors, undifferentiated by terrain type (Fig. 7), confirm results obtained previously for a similar, but smaller, sample of craters (Pike and Arthur, 1979). Morphologic features appear in fresh complex craters on Mars at different crater sizes. Flat floors, central peaks, and low d/D mark the onset of complexity in craters about 3 km to 3.5 km across. Rim-crest scalloping, accompanied by slump blocks, appears in slightly larger craters (at about 4 km diameter). The final features observed with increasing size of fresh complex craters are cratered central peaks (or central pits) and terraced rimwalls, at about 6 km to 8 km diameter. The morphologic data of Wood *et al.* (1978) for 173 fresh martian craters, when arrayed as in Fig. 7 and undifferentiated by terrain type, also are generally consistent with this ranking. The much more voluminous data of Mouginis-Mark (1979a) (compare his Fig. 7 and 8) show that central peaks occur consistently in smaller craters than do scallops and terraces (i.e., slump blocks, see Cintala *et al.*, 1977 and Wood *et al.*, 1978) up to a crater diameter of about 9 or 10 km, at which size the frequency of occurrence reverses. However, Mouginis-Mark's higher frequency of wall failure (terraces plus scallops) than central peaks above this crater diameter does not indicate a true reversal of the peaks-first trend. Rather his Fig. 8, the graph for wall failure, reflects augmenting of scallops by terraces, which my Fig. 7 shows as appearing in craters around 7 km to 8 km across.

An aside on graphic presentation is in order here. Onset diameters, which mark the first occurrence of a feature in a crater, are statistically unsound parameters of the simple-to-complex transition because (1) they only indicate the lower end of the transition range and (2) they are unique cases subject to wide variance with minor increase in the size of the sample. Accordingly, diameter/percentage-frequency curves give the most reliable transition diameters. Such diagrams are

© Lunar and Planetary Institute • Provided by the NASA Astrophysics Data System

1980LPSC...11.2159P

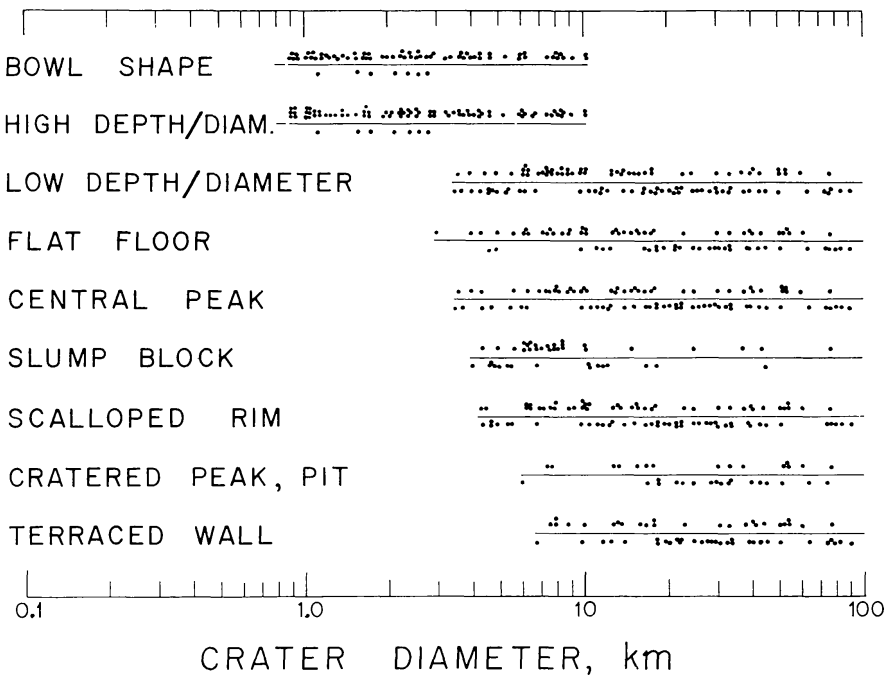

Fig. 7. Diameter/morphology arrays for nine interior characteristics of fresh martian craters. Size-dependence of crater morphology—the simple-to-complex transition—is pronounced, but terrain dependence of crater shape is more subtle (see text). Dots show unambiguous identifications of morphologic characteristics on Viking Orbiter images for most of the same 230 craters plotted in Fig. 6. Data above lines: craters on plains units (see Table 4); data below lines: craters on cratered terrain.

not given here for the data in Fig. 7, however, because the absence of large (~4–10 km across) simple craters in rough terrains would yield misleadingly different frequency curves for the occurrence of morphologic features in complex craters on the two major terrain types of Mars. This is a subtle, but crucial point, because frequency curves customarily are interpreted in terms of the appearance of *complex*-crater features. Fig. 7 shows that the occurrence of complex-crater features is the *same* on *both* terrain types; rather it is the occurrence of *simple* craters that is so different. Regardless of what technique is chosen to display and abstract the data, however, the relative order in which the features are observed in complex craters with increasing crater size remains as described in the last paragraph.

Perhaps the most important result evident in Fig. 7 is that central peaks appear in complex martian craters at smaller diameters, by a factor of two, than do terraced walls. The same relative order is clearly evident for craters on the moon (Smith and Sanchez, 1973; Wood and Andersson, 1978) and on Mercury (Cintala *et al.*, 1977; Smith and Hartnell, 1978). From the meager terrestrial data (Roddy, 1977), the sequence also may characterize meteorite craters on Earth and their experimental analogs. Together these data suggest that the first manifestations of complexity in impact craters are a flat floor, a central peak, and a low d/D ratio. Early appearance of these features is inconsistent with formation of complex craters by collapse of the transient-cavity rim into wall terraces and consequent

© Lunar and Planetary Institute • Provided by the NASA Astrophysics Data System

1980LPSC...11.2159P

deep centripetal sliding. Rather, terrace formation appears to be a later expression of complexity, not the initiating mechanism (Head, 1976; Pike, 1980).

Subdivision of the size/morphology arrays in Fig. 7 by terrain type reveals nothing that might explain the absence of large simple craters on the rough terrains or their presence on the plains, but it does suggest more possible terrain-related differences in the onset and prevalence of features within complex craters. For example, both flat floors and central-peak pits persist down to smaller crater sizes on the plains than they do in cratered terrains, an observation that agrees with the findings of Wood *et al.* (1978) and, in the case of the peak pits, with preliminary data of C. A. Hodges (pers. comm., 1980). Although central peaks and other features in Fig. 7 seem to appear at roughly the same crater sizes, Wood *et al.* (1978) found wall failure to occur more often in smaller craters on the plains. Moreover, according to the voluminous data of Mouginis-Mark (1979a, Figs. 7 and 8), central peaks and wall failure occur systematically in smaller craters in the plains than on the cratered terrains. If the latter two terrain-related contrasts are real, and do not reflect problems in obtaining a crater sample of uniform relative age from terrains of greatly varying age and roughness (e.g., Pike, 1974; Wood and Andersson, 1978), then all nine morphologic aspects of complex impact craters in Fig. 7 could be said to exhibit at least some systematic terrain-correlation (wall failure includes three aspects: slump blocks, scalloped rim crest, and terraces): namely, complex craters on Mars appear at smaller sizes on plains units than on cratered terrains.

EXTERNAL MORPHOLOGY: EJECTA

The simple-to-complex transition for internal morphology coincides with a change in the texture of ejecta surrounding fresh martian impact craters. The mechanism of ejecta emplacement seems to depend strongly on crater size (Fig. 8). Craters less than about 4 km across tend to have ejecta that displays the usual ballistic characteristics typical of craters on the moon and Mercury, whereas larger craters

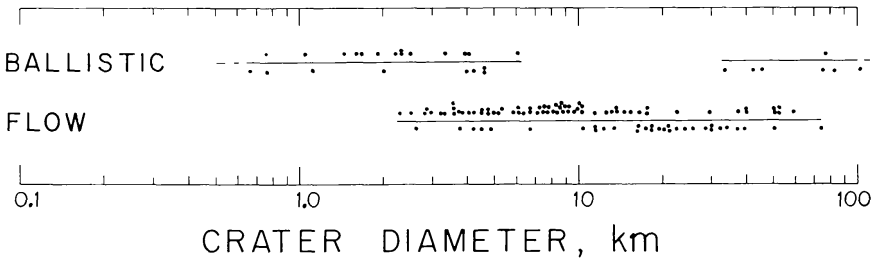

Fig. 8. Characteristic morphology of ejecta surrounding fresh impact craters on Mars. Ballistic ejecta is observed for craters 30 km $\leq$ D $\leq$ 6 km, whereas ejecta dominated by features usually ascribed to fluid flow is observed for craters 2 km $\leq$ D $\leq$ 75 km across. Overlap of the distributions about a median diameter of 4 km coincides approximately with the transition from simple to complex interior morphology. The largest craters, D $\geq$ 80 km, have mainly ballistic ejecta. For remarks on data, see Fig. 7.

© Lunar and Planetary Institute • Provided by the NASA Astrophysics Data System

1980LPSC...11.2159P

have ejecta textures that indicate a nonballistic mode of emplacement—probably by surface flow (Carr *et al.*, 1977). This 4 km-diameter threshold is close to the 5 km-diameter result obtained by Boyce (1979) for craters at the Viking Lander I site. There is similar overlap in ejecta type for both terrain types distinguished in Fig. 8, generally between crater diameters of 2.5 km and 6 km, around the median value (of overlapping craters) of 4 km, again, close to the results of Boyce (1979). The ballistic-versus-flow dichotomy in ejecta texture is not identical with the simple-to-complex contrast, however, even though the two types of changes are observed at similar crater sizes: most martian craters over 2.5 km across on plains units show evidence of flow *regardless* of whether they are simple *or* complex. Thus whatever controls formation of simple craters over 4 km across, presumably gravitational acceleration and target strength, does not necessarily control texture of the ejecta. Fluidized ejecta is thought to result from the incorporation of abundant subsurface volatiles in the cratering process (Carr *et al.*, 1977; Gault and Greeley, 1978). Detailed work by Mouginis-Mark (1979a) and by Singer and Schultz (1980) has identified other variables that may contribute to observed differences within the population of fluidized-ejecta craters on Mars.

The observations in Fig. 8 also suggest that there may be an upper size limit to fresh martian flow-ejecta craters, at a diameter of about 80 km. Identification of both ballistic and fluid-flow textures in the ejecta surrounding the fresh 55 km-diameter crater Bamberg by Mouginis-Mark (1979b) further indicates that the fluid-flow regime dominating smaller rampart craters on Mars may pass into a ballistic regime in larger craters. If these preliminary conclusions are correct, I suggest that the 4 km to 80 km size-range reflects a balance between volatile content of the target rocks, as well as depth to the volatile-rich layer, and heat released by the impact. In craters less than about 4 km across, volatile-rich strata may be too deep to be tapped by the impact (see also Boyce, 1979; Cintala and Mouginis-Mark, 1980), and in craters over 80 km across volatiles in this layer may be entirely vaporized by the great amounts of energy available. In both cases, ballistic ejecta dominate; in the latter instance, the volume of ballistic ejecta would be so much greater than that of any flow ejecta that flow features would be obscured or overwhelmed by ballistic features. Thus in neither very small nor very large craters does fluid flow dominate, a conclusion also reached by Cintala and Mouginis-Mark (1980). In the diameter range 4 km to 80 km, however, the balance between mass and depth to concentration of target volatiles and the energy level of impact may be just that required to generate the geomorphic characteristics that have been attributed to fluid flow.

With respect to texture of the ejecta, the impact craters examined in this study do not have a strong affinity for one major terrain type or the other. Craters surrounded by fluid-flow ejecta exhibit a 2:1 preference for plains units over cratered terrain (Fig. 8) but if the large simple craters, all of which fall on the plains, are ignored then the ratio drops to about 4:3. This probably is not a significant difference, particularly since flow patterns are much more difficult to see on rough terrain. Results for the two most numerous categories in Mouginis-Mark's (1979a) 1558-crater study are equally ambiguous on this score. His Type

© Lunar and Planetary Institute • Provided by the NASA Astrophysics Data System

1980LPSC...11.2159P

1 craters (single ejecta facies) are found more on cratered ("ancient") terrain than they are on cratered and smooth plains (60%:47%), but his Type 2 craters (double ejecta facies) occur in just the opposite (17%:31%) relative frequency. For the most common varieties of fluidized-ejecta craters on Mars, terrain dependence remains uncertain. More detailed work, perhaps using revised geologic units from the new geologic map of Mars (Scott, 1980), is needed.

LARGE SIMPLE CRATERS

The problem of large simple craters on Mars probably is one of explaining their absence from cratered terrains (assuming this absence is not a sampling fluke; Fig. 5) rather than their presence on the plains. This perspective follows from Fig. 2, which shows that simple craters larger than the d/D intersection are common on all planets for which both simple and complex craters have been identified. Mars is probably no exception. More detailed data for craters on the moon (Fig. 9) suggest that differences in the target, although affecting some aspects of crater shape, do not wholly preclude large simple craters from forming on one type of terrain or another. The problem for Mars may be approached by

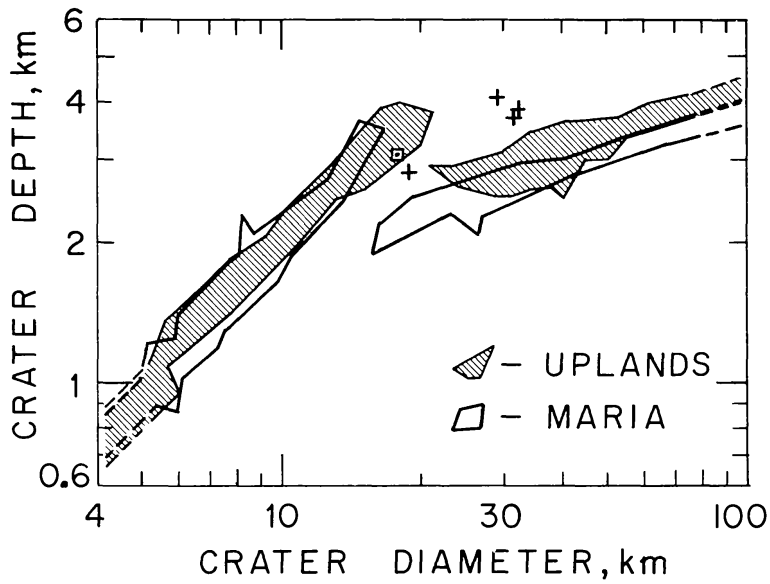

Fig. 9. Terrain-dependence of crater morphology on the moon. Depth/diameter results for 203 mare craters vs. 136 upland craters. Simple craters do not differ much in d/D (0.5%), but upland complex craters are on the average 12% deeper than mare complex craters. The simple-to-complex transition occurs on maria in craters about 16 km across, whereas it occurs in upland craters about 21 km in diameter. Square (Diophantus) and crosses (with increasing size: Dionysius, Proclus, Kant, Auzout) are craters with a morphology transitional from simple to complex configurations. To show relations in detail, plotted fields outline only craters 4.2 km ≤ D ≤ 95 km; d/D equations, revised from those in Pike (1974) using data in Pike (1976), are given in Table 2.

© Lunar and Planetary Institute • Provided by the NASA Astrophysics Data System

1980LPSC...11.2159P

examining the spatial distribution of similar-sized fresh craters on both terrain types considered here.

The 22 large simple craters (4.3 km ≤ D ≤ 10.3 km) all share a common geologic environment: young mid-latitude (16.5°N to 33.5°N) volcanic plains. Seventeen of them are concentrated in the belt between 25°N and 31°N and between longitude 228°W and 265°W, in western Elysium Planitia (Fig. 5), amid what appears to be a vast field of scattered small volcanic cones like those described by Hodges (1979). Three more craters are clustered within 200 km of each other in northeastern Chryse Planitia. One other lies 100 km west of Hecates Tholus, and another is 100 km south of Jovis Tholus. Fifteen of the craters have been excavated in unit Apc (Scott and Carr, 1978), fairly recent lava plains partly and thinly veneered with eolian sediments. Proximity of fresh volcanic constructs suggests that the lavas in which the craters formed are very young indeed. These target conditions, however, are not unique to large simple craters. Sixteen complex craters within the same size range share the same geologic environment: unit Apc. These craters lie between 5°N and 29°N, 12 of them between 23°N and 28°N. Half of them cluster to the north of Kasei Vallis, three more in Chryse Planitia, and the remaining five are disposed singly: one 300 km north of Jovis Tholus, two in Amazonis Planitia, one in Isidis Planitia, and one south of Hephaestus Fossae.

The two disparate groups of similar-sized craters do not seem to reflect apparent or inferred differences in geology, even though the complex craters all lie outside the belt of large simple craters in western Elysium Planitia (the closest being about 650 km to the south). If the Elysium concentration did not arise as the result of special target characteristics, then other alternatives, such as mass-density of impacting bodies, may be invoked. It has been proposed that simple craters formed primarily by dense meteoroids and complex craters by light meteoroids (Quaide *et al.*, 1965; Milton and Roddy, 1972; Wetherill, 1977). Could the concentration of large, deep simple craters in Elysium indicate the strewnfield of a swarm of unusually large iron-rich bolides, or is the problem one of sampling? This question cannot be answered until the locations of more large simple craters on Mars are studied, and the possibility of bias through inadequate photo coverage has been evaluated in more detail.

COMPARISON WITH EARTH AND MOON

Terrain-related contrasts in the topography of craters on the moon, which until recently have proved elusive, provide a key piece of data. Neither Quaide *et al.* (1965) nor Pike (1974) identified such a difference, but Wood and Andersson (1978) found that upland craters in their class TRI (typically 15 km ≤ D ≤ 50 km) were systematically deeper (by an average of about 18%) than those on mare surfaces. Figure 9 is a revision of my 1974 results using photogrammetric data (Pike, 1976), with some recent (unpublished) amplifications. Although simple

© Lunar and Planetary Institute • Provided by the NASA Astrophysics Data System

1980LPSC...11.2159P

craters on the maria do not differ markedly (less than half a percent) from simple upland craters in d/D (Table 2), complex upland craters 15 to 100 km across average 12% deeper than similar-sized craters on the maria (Table 2). What is even more interesting, however, is that the simple-to-complex transition on the moon occurs at a crater diameter of about 16 km on the maria and at about 21 km on the uplands (Fig. 9). This difference may correspond to the terrestrial contrast documented in Fig. 4.

The terrain-related differences in crater sizes for the transition on Earth and Moon may indicate presence or absence of significant layering in the target materials. On both planets, the smaller onset diameter occurs in demonstrably layered rocks: sandstones, shales, and limestones on Earth and mare-basalt flows on the moon. The larger onset diameter, on the other hand, is observed on both planets in what are known or inferred to be less sharply stratified materials: gneisses, schists, metavolcanics, and granites on Earth and highland breccias on the moon. These intraplanetary contrasts in D_t thus do not seem to reflect simply hard versus soft targets. Were that the case, then the transition on the moon should occur in smaller craters on the softer highland breccias than in the hard mare basalts. This is not what is observed, however, in Fig. 9.

The subtle terrain-correlated differences in size-morphology summarized here for craters on Mars suggest, tentatively, that plains materials could differ stratigraphically from those of cratered terrains. Certainly all martian terrains may be layered to some extent in that they include volatile-rich strata at depths that have affected the morphology of most impact craters over 4 km across (Boyce, 1979; Cintala and Mouginis-Mark, 1980). The difference perhaps is one of degree rather than of outright presence or absence of stratification. If the correlation between morphology and crater size that has been observed on the moon and Earth (Figs. 4 and 9) also applies to Mars, then the plains, where complex craters may occur at slightly smaller sizes than they do on cratered terrains, are inferred to be the more strongly layered of the two types of targets. The source of the enhanced stratification of plains materials could have arisen from their being successions of lava flows (perhaps intercalated with sediments), being young (and hence little reworked by impact), and being preferentially veneered by eolian and perhaps by other recent unconsolidated sediments. Further work with Viking pictures may enable these and perhaps other alternatives to be sorted out and tested.

Conrol of the simple-to-complex threshold-diameter in craters by layering of the target on Earth, Moon, and now perhaps Mars is consistent with an alternative interpretation of the D_t:g relation (Fig. 3). Rather than reflecting simply hard versus soft targets (Pike and Arthur, 1979; Pike *et al.*, 1980), deviations of the mean threshold diameter D_t from the log-log linear relation with g could indicate significant broad-scale layering in planetary crusts, as suggested by authors from Wegener (1921) to Head (1976). However, the layering itself does not necessarily trigger the formation of complex craters (Pike, 1980), and as suggested above, stratification does not always mean presence of a weak layer over a strong substrate. According to morphologic data available for craters on six solid planets and satellites, Mercury may be reinterpreted as essentially non-layered (cf. Cin-

© Lunar and Planetary Institute • Provided by the NASA Astrophysics Data System

1980LPSC...11.2159P

tala *et al.*, 1977)—perhaps the result of a planet-wide melting episode or some other type of thermal event, possibly brought about through long proximity to the sun; the earth and its moon each have both layered and non-layered—or rather strongly layered and weakly layered—portions of their crusts; and Callisto, Ganymede, and Mars are interpreted as strongly layered. Again, some of the variance in the D_t:g data in Fig. 3 may well reflect other influences not considered in detail, such as projectile characteristics, but the arguments advanced here suggest that deviation from the mean D_t:g trend could have resulted largely from the degree of target stratification.

CONCLUSIONS

The results presented in this paper, together with findings reached by other investigators, suggest that *both* gravitational acceleration *and* target characteristics have affected the morphology of impact craters across the solar system. Neither of these important influences alone can explain all of the many observations on craters. The emerging picture of morphology and process, with morphology expressed by the characteristic crater size (D_t) where the transition from simple to complex types occurs, is unclear in that the relative importance of gravity and target type differs from planet to planet. For example, intraplanetary contrasts in crater shape that reflect differences in target materials seem to be large on Earth, significant but minor on Mars and the moon, and minimal on Mercury. Whole-planet differences in crater shape between Earth and the moon, on the other hand, seem entirely dependent on g. However, the whole-planet values of D_t observed on Mercury and Mars vary from values predicted by gravity-scaling alone, an effect that may indicate strong contrasts in the surface materials of the two planets. Specific findings on crater morphology reached in this study, several of which are consistent with the results of other workers, include the following:

(1) D_t, the characteristic size that divides most fresh-appearing impact craters with a simple form from those with a complex form is determined for four planets. D_t is defined as the geometric mean of several (statistically-derived) crater diameters that express individual aspects of the simple-to-complex transition, such as changes in depth/diameter and the occurrence of central peaks.

(2) D_t is not the same for craters on each planet: ~3 km on Earth, ~6 km on Mars from a new sample of 230 craters on Viking Orbiter images, ~16 km on Mercury, and ~19 km on the moon. Preliminary estimates of D_t for Ganymede and Callisto are, respectively, ~13 km and ~15 km.

(3) Fresh impact craters vary in morphology according to the terrain on which they form on at least three planets, in decreasing order of certainty: Earth, Moon, Mars. At this time, stratification of target rocks, including the effects of volatiles, seems to explain the observations at least as well as strength *per se* of the materials.

(4) The appearance of terraces, central peaks, and other morphologic features within martian craters 3 to 8 km across occurs in a size-dependent sequence

© Lunar and Planetary Institute • Provided by the NASA Astrophysics Data System

1980LPSC...11.2159P

resembling that observed for craters on the moon. Only the crater size at which the simple-to-complex transition occurs, D_t, is different (cf. Wood *et al.*, 1978). The sequence, in which central peaks are observed in smaller craters than are rimwall terraces, is not consistent with formation of complex craters by centripetal slump and deep sliding of rim terraces (cf. Head, 1976; Pike, 1980).

(5) Occurrence of the transition on both martian plains and cratered terrain in smaller craters ($D_t \simeq 6$ km) than would be expected from the inverse statistical relation between D_t and g alone ($D_t \simeq 9$ km) shows that some other influence applies. Comparison of similar morphologic data for craters on different terrains of Earth and the moon suggests that all martian terrains may be significantly stratified.

(6) The morphologic transition may occur at a slightly smaller crater size on martian plains than on the cratered terrains, a difference I ascribe to plains materials being more highly stratified (cf., Wood *et al.*, 1978).

(7) Complex craters on both the moon and Mars exhibit marked terrain-related differences in d/D, whereas simple craters do not. Complex martian craters in rough terrains average 13 percent deeper than plains craters. Revision of the lunar d/D relation reveals a similar terrain-correlated difference: the morphologic transition occurs in slightly smaller craters on the maria than it does in upland craters, a result of upland craters being significantly (an average of 12 percent) deeper than those on the maria (cf., Wood and Andersson, 1978).

(8) Cratered terrains on Mars may be deficient in large simple impact craters ($3.5 \text{ km} \leq D \leq 10 \text{ km}$). Other than acknowledging a possible sampling deficiency, at this time I have no firm explanation for the observation that 17 of the 22 large simple craters examined here are localized in western Elysium Planitia.

(9) A change from ballistic to fluid-flow ejecta occurs in martian craters on both plains and cratered terrains at about 4 km diameter (cf., Boyce, 1979). The difference is not necessarily related to the simple-to-complex transition in interior morphology. A second change in ejecta texture, back to a mainly ballistic regime for craters over 80 km across, suggests that the quantity of crustal volatiles that can become involved in an impact may have a finite limit (cf., Cintala and Mouginis-Mark, 1980).

(10) Preliminary determinations of the simple-to-complex transition for craters on Callisto and Ganymede are consistent with either low target strength or significant layering in the rocks of these bodies. Crustal volatiles are important in either case. Conversely, Mercury is inferred to be either a very strong target, stronger than the moon, or else to have nonlayered (and dry) rocks at the surface (cf., Cintala *et al.*, 1977).

(11) The first d/D results for what appear to be large impact craters on Venus (reported in Kerr, 1980) lie just below the d/D trend for ringed complex craters on Earth. More data are needed before interpreting this possible coincidence in terms of the overall D_t:g model proposed here.

The most fruitful area for further research in crater morphology now lies in ascertaining the relative importance of gravity and target type on each planet, rather than in attempting to ascribe all morphologic observations to either one

© Lunar and Planetary Institute • Provided by the NASA Astrophysics Data System

1980LPSC...11.2159P

competing explanation or the other. Another related problem is whether or not variations in velocity and/or mass-density of the impacting projectiles might better explain some of the morphologic data. Finally, detailed observations of craters on Venus, Ganymede, Callisto, and perhaps the larger satellites of Saturn will test some of the ideas discussed or proposed here.

Acknowledgments—Supported by NASA Geology Programs office. Mike Carr and Dai Arthur brought to my attention the many intricacies of Viking Orbiter images and their processing. I am indebted to Karl Blasius, Mike Carr, Mark Cintala, and Hank Moore for reviews that substantially improved the presentation. This paper is dedicated to the memory of Alfred Wegener, insightful investigator of crater morphology, on the occasion of the 100th anniversary of his birth.

REFERENCES

Baldwin R. B. (1949) *The Face of the Moon*. Univ. Chicago Press, Chicago. 239 pp.

Boyce J. M. (1979) A method for measuring heat flow in the martian crust using impact crater morphology. Repts. Planetary Geol. Program 1978–1979, NASA TM 80339, p. 114–118.

Carr M. H., Crumpler L. S., Cutts J. A., Greeley R., Guest J. E., and Masursky H. (1977) Martian impact craters and emplacement of ejecta by surface flow. *J. Geophys. Res.* **82,** 4055–4065.

Cintala M. J. (1979) Mercurian crater rim heights and some interplanetary comparisons. *Proc. Lunar Planet. Sci. Conf. 10th,* p. 2635–2650.

Cintala M. J. and Mouginis-Mark P. J. (1980) Martian fresh carter depths: More evidence for substrate volatiles? (abstract). In *Lunar and Planetary Science XI,* p. 143–145. Lunar and Planetary Institute, Houston.

Cintala M. J., Wood C. A., and Head J. W. (1977) The effects of target characteristics on fresh crater morphology: Preliminary results for the moon and Mercury. *Proc. Lunar Sci. Conf. 8th,* p. 3409–3425.

Cooper H. F. (1977) A summary of explosion cratering phenomena relevant to meteor impact events. In *Impact and Explosion Cratering* (D. J. Roddy, R. O. Pepin, and R. B. Merrill, eds.), p. 11–44. Pergamon, N. Y.

Dence M. R. (1964) A comparative structural and petrographic study of probable Canadian meteorite craters. *Meteoritics* **2,** 249–270.

Dence M. R. (1972) The nature and significance of terrestrial impact structures. *International Geological Congress, XXIV Session, Section 15,* p. 77–89.

Gault D. E. and Greeley R. (1978) Exploratory experiments of impact craters formed in viscous-liquid targets: Analogs for martian rampart craters? *Icarus* **34,** 486–495.

Gault D. E., Guest J. E., Murray J. B., Dzurisin D., and Malin M. C. (1975) Some comparisons of impact craters on Mercury and the moon. *J. Geophys. Res.* **80,** 2444–2460.

Gilbert G. K. (1893) The Moon's face; a study of the origin of its features. *Bull. Phil. Soc. Wash.* **12,** 241–292.

Gordin V. M., Dabizha A. I., Krass M. S., Mikhailov V. O., and Myasnikov V. P. (1979) Geophysical and geomechanical aspects of the study of meteorite structures. *Phys. Earth Planet. Inter.* **20,** 1–11.

Grieve R. A. F. and Robertson P. B. (1979) The terrestrial cratering record I. Current Status of observations. *Icarus* **38,** 212–229.

Hartmann W. K. (1972) Interplanet variations in scale of crater morphology—Earth, Mars, Moon. *Icarus* **17,** 707–713.

Hartmann W. K. (1977) Relative crater production rates on planets. *Icarus* **31,** 260–276.

Hawke B. R. and Head J. W. (1977) Impact melt on lunar crater rims. In *Impact and Explosion Cratering* (D. J. Roddy, R. O. Pepin, and R. B. Merrill, eds.), p. 815–841. Pergamon, N. Y.

© Lunar and Planetary Institute • Provided by the NASA Astrophysics Data System

1980LPSC...11.2159P

Head J. W. (1976) The significance of substrate characteristics in determining morphology and morphometry of lunar craters. *Proc. Lunar Sci. Conf. 7th*, p. 2913–2929.

Hodges C. A. (1979) Some lesser volcanic provinces on Mars. Repts. Planetary Geol. Program 1978–1979, NASA TM 80339, p. 247–249.

Johansen L. A. (1979) The latitude dependence of martian splosh cratering and its relationship to water. Repts. Planetary Geol. Program 1978–1979, NASA TM 80339, p. 123–125.

Johnson T. V. (1978) The galilean satellites of Jupiter: Four worlds. *Ann. Rev. Earth Planet. Sci.* **6**, 93–125.

Kerr R. A. (1980) Venus: Not simple or familiar, but interesting. *Science* **207**, 289–293.

Kieffer S. W. and Simonds C. H. (1980) The role of volatiles and lithology in the impact cratering process. *Rev. Geophys. Space Phys.* **18**, 143–181.

Mackin J. H. (1969) Origin of lunar maria. *Bull. Geol. Soc. Amer.* **80**, 735–748.

Malin M. C. and Dzurisin D. (1977) Landform degradation on Mercury, the moon, and Mars: Evidence from crater depth/diameter relationships. *J. Geophys. Res.* **82**, 376–388.

Malin M. C. and Dzurisin D. (1978) Modification of fresh crater landforms: evidence from the moon and Mercury. *J. Geophys. Res.* **83**, 233–243.

Milton D. J., Barlow B. C., Brett R., Brown A. R., Glikson A. Y., Manwaring F. A., Moss F. J., Sedmik E. C., Van Son J., and Young G. A. (1972) Gosses Bluff impact structure, Australia. *Science* **175**, 1199–1207.

Milton D. J. and Roddy D. J. (1972) Displacements within impact craters. *International Geological Congress, XXIV Session, Section 15*, p. 119–124.

Morrison D. and Cruikshank D. P. (1974) Physical properties of the natural satellites. *Space Sci. Rev.* **15**, 641–739.

Mouginis-Mark P. J. (1979a) Martian fluidized crater morphology: Variations with crater size, latitude, altitude, and target material. *J. Geophys. Res.* **84**, 8011–8022.

Mouginis-Mark P. J. (1979b) Ejecta emplacement of the martian impact crater Bamburg. *Proc. Lunar Planet. Sci. Conf. 10th*, p. 2651–2668.

Mutch T. A., Arvidson R. E., Head J. W., Jones K. L., and Saunders R. S. (1976) *The Geology of Mars*. Princeton Univ. Press, N. J. 400 pp.

Oberbeck V. R. and Quaide W. L. (1967) Estimated thickness of a fragmental layer of Oceanus Procellarum. *J. Geophys. Res.* **72**, 4697–4704.

Pike R. J. (1974) Depth/diameter relations of fresh lunar craters: revision from spacecraft data. *Geophys. Res. Lett.* **1**, 291–294.

Pike R. J. (1975) Size-morphology relations of lunar craters: Discussion. *Mod. Geol.* **5**, 169–173.

Pike R. J. (1976) Crater dimensions from Apollo data and supplemental sources. *The Moon* **12**, 463–477.

Pike R. J. (1977) Size-dependence in the shape of fresh impact craters on the moon. In *Impact and Explosion Cratering* (D. J. Roddy, R. O. Pepin, and R. B. Merrill, eds.), p. 489–509. Pergamon, N. Y.

Pike R. J. (1980) Formation of complex impact craters: Evidence from Mars and other planets. *Icarus*. In press.

Pike R. J. and Arthur D. W. G. (1979) Simple to complex impact craters: The transition on Mars. Repts. Planetary Geol. Program 1978–1979, NASA TM-80339, p. 132–134.

Pike R. J., Roddy D. J., and Arthur D. W. G. (1980) Gravity and target strength: Controls on the morphologic transition from simple to complex impact craters. Repts. Planetary Geol. Program 1979–1980, NASA TM 81776, p. 108–110.

Quaide W. L., Gault D. E., and Schmidt R. A. (1965) Gravitative effects on lunar impact structures. *Ann. N. Y. Acad. Sci.* **123**, p. 563–572.

Roddy D. J. (1977) Large-scale impact and explosion craters: Comparisons of morphological and structural analogs. In *Impact and Explosion Cratering* (D. J. Roddy, R. O. Pepin, and R. B. Merrill, eds.), p. 185–246. Pergamon Press, N. Y.

Roddy D. J. (1979) Structural deformation at the Flynn Creek impact crater, Tennessee: A preliminary report on deep drilling. *Proc. Lunar Planet. Sci. Conf. 10th*, p. 2519–2534.

© Lunar and Planetary Institute • Provided by the NASA Astrophysics Data System

1980LPSC...11.2159P

Sabaneyev P. F. (1962) Some results deduced from simulations of lunar craters. In *The Moon* (Z. Kopal and Z. K. Mikhailov, eds.), p. 419–431. Academic, N. Y.

Schultz P. H. (1976) *Moon Morphology*. Univ. Texas Press, Austin. 626 pp.

Scott D. H. (1980) Mars geologic map, 1:15 million scale. Repts. Planetary Geol. Program, NASA TM 81776, p. 372.

Scott D. H. and Carr M. H. (1978) Geologic map of Mars. U. S. Geol. Survey Misc. Geol. Inv. Map I–1083.

Singer J. and Schultz P. H. (1980) Secondary impact craters around lunar, mercurian, and martian craters (abstract). In *Lunar and Planetary Science XI,* p. 1042–1044. The Lunar and Planetary Institute, Houston.

Smith E. I. and Hartnell J. A. (1978) Crater size-shape profiles for the moon and Mercury: Terrain effects and interplanetary comparisons. *The Moon and Planets* **19,** 479–511.

Smith E. I. and Sanchez A. G. (1973) Fresh lunar craters: Morphology as a function of diameter, a possible criterion for crater origin. *Mod. Geol.* **4,** 51–59.

Smith B. A., Soderblom L. A., Johnson T. V., Ingersoll A. P., Collins S. A., Shoemaker E. M., Hunt G. E., Masursky H., Carr M. H., Davies M. E., Cook A. F. II, Boyce J., Danielson G. E., Owen T., Sagan C., Beebe R. F., Veverka J., Strom R. G., McCauley J. F., Morrison D., Briggs G. A., and Suomi V. E. (1979a) The Jupiter system through the eyes of Voyager 1. *Science* **204,** 951–972.

Smith B. A., Soderblom L. H., Beebe R., Boyce J., Briggs G., Carr M., Collins S. A., Cook A. F. II, Danielson G. E., Davies M. E., Hunt G. E., Ingersoll A., Johnson T. V., Masursky H., McCauley J., Morrison D., Owen T., Sagan C., Shoemaker E. M., Strom R., Suomi V. E., and Veverka J. (1979b) The Galilean satellites and Jupiter: Voyager 2 imaging science results. *Science* **206,** 927–950.

Thomas P. C. (1978) *The Morphology of Phobos and Deimos*. Ph.D. thesis, Cornell Univ., Ithaca, N. Y. 272 pp.

von Englehardt W., Bertsch W., Stöffler D., Groschopf P., and Reiff W. (1967) Anzeichen für meteoritischen Ursprung des Beckens von Steinheim. *Naturwissenschaften* **54,** 198–199.

Wegener A. (1921) Die Entstehung der Mondkrater. Braunschweig, Sammlung Vieweg, Tayesfragen. *Natur. u. Tech.* **55,** 48 pp.

Wetherill G. W. (1977) The nature of the present interplanetary crater-forming projectiles. In *Impact and Explosion Cratering* (D. J. Roddy, R. O. Pepin, and R. B. Merrill, eds.), p. 613–615. Pergamon, N. Y.

Wilshire H. G., Offield T. W., Howard K. A., and Cummings D. (1972) Geology of the Sierra Madera cryptoexplosion structure, Pecos County, Texas. *U. S. Geol. Survey Prof. Paper 599-H,* 42 pp.

Wood C. A. and Andersson L. (1978) New morphometric data for fresh lunar craters. *Proc Lunar Planet. Sci. Conf. 9th,* p. 3669–3689.

Wood C. A., Head J. W., and Cintala M. J. (1978) Interior morphology of fresh martian craters: The effects of target characteristics. *Proc. Lunar Planet. Sci. Conf. 9th,* p. 3691–3709.

© Lunar and Planetary Institute • Provided by the NASA Astrophysics Data System